

# Thermal Radiation and Chemical Reaction Effects on Steady Convective Slip Flow with Uniform Heat and Mass Flux in the Presence of Ohmic Heating and a Heat Source

Gnaneswara Reddy Machireddy<sup>1</sup>

**Abstract:** This study deals with the investigation of the effects exerted by heat radiation and a first-order chemical reaction on the magnetohydrodynamics boundary layer slip flow which is established past a vertical permeable surface embedded in a porous medium (with uniform heat and mass flux). The heat equation includes the relevant terms, i.e. the viscous dissipation, radiative heat flux, Ohmic dissipation, and absorption of radiation. The mass transfer equation takes into account the effects related to the chemically reactive species. A classical model for optically thin media is used for studying the effect of radiation. The resulting non-linear coupled partial differential equations are solved by a perturbation technique. The results show that the velocity, temperature and concentration fields are appreciably influenced by the presence of chemical reactions, thermal stratification and the imposed magnetic field. The effects of various parameters on the skin-friction coefficient are also assessed.

**Keywords:** Thermal radiation, MHD, Ohmic heating, Slip flow, Chemical reaction, Uniform heat and mass flux.

## 1 Introduction

Convective flow with simultaneous heat and mass transfer under the influence of a magnetic field and a chemical reaction have attracted a considerable attention of researchers because such processes exist in many branches of science and technology. Possible applications of this type of flow can be found in many industries viz. in the chemical industry, cooling of nuclear reactors and magnetohydrodynamic (MHD) power generators. Free convection flow occurs frequently in nature. It occurs not only due to temperature difference, but also due to concentration difference or combination of these two. Many transport processes exist in industrial applications in

---

<sup>1</sup> Department of Mathematics, Acharya Nagarjuna University Ongole Campus, Ongole, A.P. (India)-523 001. E-Mail: mgrmaths@gmail.com

which the simultaneous heat and mass transfer occur as a result of combined buoyancy effects of diffusion of chemical species. Free convection flows in a porous media with chemical reaction have wide applications in geothermal and oil reservoir engineering as well as in chemical reactors of porous structure. Moreover, considerable interest has been evinced in radiation interaction with convection and chemical reaction for heat and mass transfer in fluids. This is due to the significant role of thermal radiation in the surface heat transfer when convection heat transfer is small, particularly, in free convection problems involving absorbing–emitting fluids. Khair and Bejan (1985) studied heat and mass on flows past an isothermal flat plate. Lin and Wu (1995) analyzed combined heat and mass transfer by laminar natural convection from a vertical plate. Yin (1999) studied numerically the free convection effect on magnetohydrodynamics heat and mass transfer of a continuously moving permeable surface. Acharya et al. (1999) have studied heat and mass transfer over an accelerating surface with heat source in the presence of suction and blowing. Gnanaswara Reddy and Bhaskar Reddy (2011) analyzed the mass transfer and heat generation effects on MHD free convection flow past an inclined vertical surface in a porous medium.

It is well known that the boundary condition for a viscous fluid at a solid wall obeys no-slip condition, i.e., the fluid velocity matches the velocity of the solid boundary. However, in many practical applications, the particle adjacent to a permeable surface no longer takes the velocity of the surface but the particle at the surface has a finite tangential velocity which slips along the surface. The flow regime is called a slip-flow regime, and this effect cannot be neglected. Sharma and Chaudhury (2003) studied the effect of variable suction on transient free convective viscous incompressible flow past a vertical plate in a slip-flow regime. Hayat et al. (2002) investigated the flow of an elasto-viscous fluid past an infinite wall with time-dependent suction.

Many processes in new engineering areas take place at high temperatures and knowledge of radiation heat transfer becomes very important for the design of the pertinent equipment. Recent developments in hypersonic flights, nuclear power plant gas turbines and various propulsion devices for aircraft, missiles, satellites and space vehicles have focused attention of researchers on thermal radiation as a mode of energy transfer, and emphasized the need for inclusion of radiative transfer in these processes. The study of radiation effects on the various types of flow is quite complicated. The interaction of radiation with mixed convection flow past a vertical plate was investigated by Hossain and Takhar (1996). Seddeek (2002) examined the effect of radiation and variable viscosity on unsteady force convection flows in the presence of an align magnetic field. Aydin and Kaya (2008) studied the effect of radiation on MHD mixed convection flow about a permeable vertical

plate. Gnanaswara Reddy (2012) analyzed Thermal radiation and viscous dissipation effects on MHD marangoni convection flow over a permeable flat surface with heat generation/absorption. Very recently, Gnanaswara Reddy (2013) investigated the influence of thermal radiation, viscous dissipation and hall current on MHD convection flow over a stretched vertical flat plate.

In order to transform cheaper raw materials to high value products, the raw materials are made to undergo chemical reaction in all industrial chemical process. Such chemical transformations take place in a reactor. The reactor plays an important role of bringing reactants into intimate contact and providing an appropriate environment for adequate time and allowing the removal of finished products. Thus we are particularly interested in cases in which diffusion and chemical reaction occur at roughly the same speed. The study of heat generation or absorption effects in moving fluids is important in view of several physical problems such as fluids undergoing exothermic or endothermic chemical reactions. Thus in many industrial processes involving flow and mass transfer over a moving surface, the diffusing species can be generated or absorbed due to some kind of chemical reaction with the ambient fluid which can greatly affect the flow and hence the properties and quality of the final product. Processes involving the mass transfer effect have long been recognized as important principally in chemical processing equipments. Kandasamy et al. (2005) investigated the effects of chemical reaction, heat source and thermal stratification on heat and mass transfer in MHD flow over a vertical stretching surface. Ghaly and Seddeek (2004) have investigated the effect of chemical reaction, heat and mass transfer on laminar flow along a semi-infinite horizontal plate with temperature dependent viscosity. Recently, Gnanaswara Reddy (2013) studied chemically reactive species and radiation effects on MHD convective flow past a moving vertical cylinder.

In all the above investigations, the effect of Ohmic heating are not considered in the problem of coupled heat and mass transfer in the presence of magnetic field. However, it is more realistic to include Ohmic effect in order to explore the impact of the magnetic field on the thermal transport in the boundary layer. The effect of Ohmic heating on the MHD free convective heat transfer has been examined by Hossain (1992) for a Newtonian fluid. Abo-Eldahab and Abd El-Aziz (2004) studied the effect of Ohmic heating on mixed convection boundary layer flow of a micropolar fluid from a rotating cone by considering power law variation in surface temperature. Chaudhary et al. (2006) have analyzed the effect of radiation on heat transfer in MHD mixed convection flow with simultaneous thermal and mass diffusion from an infinite vertical plate with viscous dissipation and Ohmic heating. Abd El-Aziz (2007) studied the effect of Ohmic heating on combined heat and mass transfer of viscous incompressible fluid having temperature dependent viscosity as

well as thermal conductivity in MHD three-dimensional flow over a stretching surface. The problem of combined heat and mass transfer of an electrically conducting fluid in MHD natural convection adjacent to a vertical surface is analyzed by Chen (2004) by taking into account the effects of Ohmic heating and viscous dissipation but neglected chemical reaction of the species. Very recently, thermal radiation and chemical reaction effects on MHD mixed convective boundary layer slip flow in a porous medium with heat source and Ohmic heating is analyzed by Gnanaswara Reddy (2014).

Thus the present investigation is concerned with the study of MHD and Ohmic heating in steady two-dimensional boundary layer slip flow of a viscous incompressible dissipating fluid past a vertical permeable plate with the diffusion of species in the presence of thermal radiation incorporating first-order chemical reaction with uniform heat and mass flux. The classical model introduced by Cogley et al. (1968) is used for the radiation effect as it has the merit of simplicity and enables us to introduce linear term in temperature in the analysis for optically thin media. The effects of various physical parameters on the velocity, temperature and concentration profiles as well as on local skin-friction coefficient are discussed. Validation of the analysis has been performed by comparing the present results with those available in the open literature (2000) and a very good agreement has been established.

## 2 Mathematical Formulation

Consider the steady two-dimensional laminar boundary layer flow of a viscous incompressible electrically conducting and heat absorbing fluid past a semi-infinite vertical permeable plate embedded in a uniform porous medium which is subject to slip boundary condition, uniform heat and mass flux. The  $x^*$ -axis is along the plate and  $y^*$  is perpendicular to the plate. It is assumed that there exists a homogeneous chemical reaction of first-order with rate constant  $R$  between the diffusing species and the fluid. The concentration of the diffusing species is very small in comparison to other chemical species, the concentration of species far from the wall,  $C_\infty$ , is infinitesimally small and hence the Soret and Dufour effects are neglected. The chemical reactions are taking place in the flow and all thermo-physical properties are assumed to be constant except density in the buoyancy terms of the linear momentum equation which is approximated according to the Boussinesq approximation. It is also assumed that viscous and electrical dissipation are negligible. A uniform transverse magnetic field of magnitude  $B_0$  is applied in the presence of radiation and concentration buoyancy effects in the direction of  $y^*$ -axis. The transversely applied magnetic field and magnetic Reynolds number are assumed to be very small so that the induced magnetic field and the Hall effect are negligible. It is assumed that the porous medium is homogeneous and present everywhere in

local thermodynamic equilibrium. Rest of properties of the fluid and the porous medium are assumed to be constant. The governing equations for this investigation are based on the balances of mass, linear momentum, energy and concentration species. Taking into consideration these assumptions, the equations that describe the physical situation can be written in Cartesian frame of references, as follows:

Continuity Equation:

$$\frac{dv^*}{dy^*} = 0 \tag{1}$$

i.e.  $v^* = -v_0$  (Constant) (2)

$$\frac{dp^*}{dy^*} = 0 \Rightarrow p^* \text{ is independent of } y^* \tag{3}$$

Momentum Equation:

$$\rho v^* \frac{du^*}{dy^*} = \mu \frac{d^2u^*}{dy^{*2}} + g\beta(T^* - T_\infty) + g\beta^*(C^* - C_\infty) - \sigma B_0^2 u^{*2} - \frac{\mu}{K^*} u^* \tag{4}$$

Energy Equation:

$$\rho c_p v^* \frac{dT^*}{dy^*} = \alpha \frac{d^2T^*}{dy^{*2}} + \mu \left( \frac{du^*}{dy^*} \right)^2 - \frac{\partial q_r^*}{\partial y^*} + \sigma B_0^2 u^{*2} - Q_0(T^* - T_\infty) + Q_1^*(C^* - C_\infty) \tag{5}$$

Mass Diffusion Equation:

$$v^* \frac{dC^*}{dy^*} = D \frac{d^2C^*}{dy^{*2}} - R(C^* - C_\infty) \tag{6}$$

where  $x^*$ ,  $y^*$  are the dimensional distances along and perpendicular to the plate, respectively.  $g$  is the gravitational acceleration,  $T^*$  is the dimensional temperature of the fluid near the plate,  $T_\infty$  is the free stream dimensional temperature,  $K^*$  is the permeability of the porous medium,  $C^*$  is the dimensional concentration,  $C_\infty$  is the free stream dimensional concentration.  $\beta$  and  $\beta^*$  are the thermal and concentration expansion coefficients, respectively.  $p^*$  is the pressure,  $c_p$  is the specific heat of constant pressure,  $\mu$  is viscosity of the fluid,  $q_r^*$  is the radiative heat flux,  $\rho$  is the density,  $\sigma$  is the magnetic permeability of the fluid,  $v_0$  is the constant suction velocity,  $v$  is the kinematic viscosity,  $D$  is the molecular diffusivity,  $Q_0$  is the dimensional heat absorption coefficient,  $Q_1^*$  is the coefficient of proportionality of the absorption of the radiation and  $R$  is the chemical reaction parameter.  $u^*$  and  $v^*$  are the components of dimensional velocities along  $x^*$  and  $y^*$  directions, respectively,  $\alpha$  is

the fluid thermal diffusivity. The second and third terms on RHS of the momentum equation (4) denote the thermal and concentration buoyancy effects, respectively. Also second and fourth terms on the RHS of energy equation (5) represents the viscous dissipation and Ohmic dissipation, respectively. The third and fifth term on the RHS of Eq. (5) denote the inclusion of the effect of thermal radiation and heat absorption effects, respectively.

The radiative heat flux is given by [Cogley, Vincenty and Gilles (1968)]

$$\frac{\partial q_r^*}{\partial y^*} = 4(T^* - T_\infty)I' \tag{7}$$

where  $I' = \int_0^\infty K_{\lambda w} \frac{\partial e_{b\lambda}}{\partial T^*} d\lambda$ ,  $K_{\lambda w}$  is the absorption coefficient at the wall and  $e_{b\lambda}$  is Planck's function.

Under these assumptions, the appropriate boundary conditions for velocity involving slip flow, temperature and concentration fields are defined as

$$u^* = u_{slip}^* = \frac{\sqrt{k_1}}{\alpha_1} \frac{du^*}{dy^*}, \quad \frac{\partial T^*}{\partial y} = -\frac{q'}{k}, \quad \frac{\partial C^*}{\partial y} = -\frac{j''}{D} \quad \text{at } y = 0 \tag{8}$$

$$u^* \rightarrow 0, \quad T^* \rightarrow T_\infty, \quad C^* \rightarrow C_\infty \quad \text{as } y \rightarrow \infty \tag{9}$$

where  $C_w$  and  $T_w$  are the wall dimensional concentration and temperature, respectively.  $k_1$  is the permeability of the porous medium,  $\alpha_1$  is the porous parameter,  $k$  is the thermal conductivity  $q'$  is the constant heat flux at the plate and  $j''$  is the mass flux per unit area.

Introducing the following non-dimensional quantities

$$y = \frac{v_0 y^*}{\nu}, \quad u = \frac{u^*}{v_0}, \quad Gr = \frac{g\beta v^2 \left(\frac{q'}{kv_0}\right)}{v_0^3}, \quad Gm = \frac{g\beta^* v^2 \left(\frac{j''}{Dv_0}\right)}{v_0^3}, \quad M^2 = \frac{\sigma B_0^2 v^2}{v_0^2 \mu},$$

$$K = \frac{K^* v_0^2}{\nu^2}, \quad Pr = \frac{\mu c_p}{\alpha}, \quad F = \frac{4\nu I'}{\rho c_p v_0^2}, \quad \varphi = \frac{Q_0 \nu}{\rho c_p v_0^2}, \quad Q_1 = \frac{Q_1^* \nu (C_w - C_\infty)}{v_0^2 (T_w - T_\infty)}, \tag{10}$$

$$E = \frac{v_0^2}{c_p (T_w - T_\infty)}, \quad \theta = \frac{T^* - T_\infty}{(q' v^2 / kv_0)}, \quad C = \frac{C^* - C_\infty}{(j'' v^2 / Dv_0)}, \quad Sc = \frac{\nu}{D}, \quad \gamma = \frac{R\nu}{v_0^2}$$

Using (7) and (10) in Eqs. (4)–(6), we get the following non-dimensional equations:

$$\frac{d^2 u}{dy^2} + \frac{du}{dy} + Gr\theta + Gm\varphi - \left(M^2 + \frac{1}{K}\right)u = 0 \tag{11}$$

$$\frac{d^2\theta}{dy^2} + \text{Pr} \frac{d\theta}{dy} + \text{Pr} E \left( \frac{du}{dy} \right)^2 - \text{Pr} (F + \varphi) \theta + \text{Pr} E M^2 u^2 + Q_1 C = 0 \tag{12}$$

$$\frac{d^2C}{dy^2} + \text{Sc} \frac{dC}{dy} - \text{Sc} \gamma C = 0 \tag{13}$$

where  $Gr$  is the Grashof number,  $Gm$  is the solutal Grashof number,  $\text{Pr}$  is the Prandtl number,  $M$  is the magnetic field parameter,  $F$  is the radiation parameter,  $\text{Sc}$  is the Schmidt number,  $E$  is the Eckert number,  $\varphi$  is the heat source parameter,  $\gamma$  is the chemical reaction parameter,  $K$  is the permeability parameter and  $Q_1$  is the absorption of radiation parameter.

The corresponding boundary condition (8) and (9) in dimensionless form are

$$u = u_{slip} = h \frac{du}{dy}, \quad \frac{\partial \theta}{\partial y} = -1, \quad \frac{\partial C}{\partial y} = -1 \quad \text{at } y = 0 \tag{14}$$

$$u \rightarrow 0, \quad \theta \rightarrow 0, \quad C \rightarrow 0 \quad \text{as } y \rightarrow \infty \tag{15}$$

where  $h = \frac{\sqrt{k_1} v_0^2}{\alpha_1 v}$  is the rarefaction parameter.

### 3 Method of solution

It is difficult to obtain the closed-form solution of a set of coupled ordinary differential Eqs. (11)–(13). However, these equations can be solved analytically after reducing them to a set of ordinary differential equations in dimensionless form. Thus we can represent the velocity  $u$ , temperature  $\theta$  and concentration  $C$  in terms of power of Eckert number  $E$  as in the flow of an incompressible fluid Eckert number is always less than unity since the flow due to the Joules dissipation is super imposed on the main flow. Hence, we can assume

$$u(y) = u_0(y) + E u_1(y) + O(E^2), \tag{16}$$

$$\theta(y) = \theta_0(y) + E \theta_1(y) + O(E^2), \tag{17}$$

$$C(y) = C_0(y) + E C_1(y) + O(E^2), \tag{18}$$

Substituting (16)–(18) in Eqs. (11)–(13) and equating the coefficient of zeroth powers of  $E$  (i.e.  $O(E^0)$ ), we get the following set of equations:

$$u_0'' + u_0' + Gr \theta_0 + Gm C_0 - p u_0 = 0 \tag{19}$$

$$\theta_0'' + \text{Pr} \theta_0' - \text{Pr} (F + \varphi) \theta_0 + \text{Pr} Q_1 C_0 = 0 \tag{20}$$

$$C_0'' + \text{Sc} C_0' - \text{Sc} \gamma C_0 = 0 \tag{21}$$

Next, equating the coefficients of first-order of  $E$  (i.e.  $O(E^1)$ ), we obtain

$$u_1'' + u_1' + Gr\theta_1 + GmC_1 - pu_1 = 0 \tag{22}$$

$$\theta_1'' + Pr\theta_1' - Pr(F + \varphi)\theta_1 + Pru_0^2 + PrM^2u_0^2 + PrQ_1C_1 = 0 \tag{23}$$

$$C_1'' + ScC_1' - Sc\gamma C_1 = 0 \tag{24}$$

where  $p = (M^2 + \frac{1}{K})$  and the corresponding boundary conditions are

$$u_0 = hu_0', u_1 = hu_1', \theta_0' = -1, \theta_1' = 0, C_0' = -1, C_1' = 0 \text{ at } y = 0 \tag{25}$$

$$u_0 \rightarrow 0, u_1 \rightarrow 0, \theta_0 \rightarrow 0, \theta_1 \rightarrow 0, C_0 \rightarrow 0, C_1 \rightarrow 0 \text{ as } y \rightarrow \infty \tag{26}$$

Solving Eqs. (19)–(24) with the help of boundary conditions (25) and (26), we get

$$u_0 = A_7e^{-A_4y} + A_5e^{-A_2y} + A_6e^{-A_1y} \tag{27}$$

$$\theta_0 = \left( \frac{1 - A_1A_3}{A_2} \right) e^{-A_2y} + A_3e^{-A_1y} \tag{28}$$

$$C_0 = \frac{1}{A_1}e^{-A_1y} \tag{29}$$

$$u_1 = A_{27}e^{-A_4y} + A_{15}e^{-A_2y} + A_{16}e^{-2A_1y} + A_{17}e^{-2A_2y} + A_{18}e^{-2A_4y} + A_{19}e^{-(A_1+A_2)y} + A_{20}e^{-(A_1+A_4)y} + A_{21}e^{-(A_2+A_4)y} \tag{30}$$

$$\theta_1 = A_{14}e^{-A_2y} + A_8e^{-2A_1y} + A_9e^{-2A_2y} + A_{10}e^{-2A_4y} + A_{11}e^{-(A_1+A_2)y} + A_{12}e^{-(A_1+A_4)y} + A_{13}e^{-(A_2+A_4)y} \tag{31}$$

$$C_1 = 0 \tag{32}$$

where  $A$ 's are given in Appendix A.

The skin-friction coefficient is an important physical parameter for this type of boundary layer flow which are defined and determined as follows:

$$C_{fx} = \frac{\tau_w}{\rho v_0^2} = \left. \frac{\partial u}{\partial y} \right|_{y=0}$$

$$C_{fx} = - \left[ A_4A_7 + A_2A_5 + A_1A_6 + E \left( A_4A_{27} + A_2A_{15} + 2A_1A_{16} + 2A_2A_{17} + 2A_4A_{18} + A_{19}(A_1 + A_2) + A_{20}(A_1 + A_4) + A_{21}(A_2 + A_4) \right) \right] \tag{33}$$

#### 4 Results and discussions

The present paper deals with the problem of combined effect of MHD and Ohmic heating in steady two-dimensional boundary layer slip flow of a viscous incompressible dissipating fluid past a vertical permeable plate with the diffusion of species in the presence of thermal radiation incorporating first-order chemical reaction with uniform heat and mass flux. The solutions for velocity field, temperature and concentration fields are obtained using perturbation technique. The effects of various physical parameters such as thermal Grashof number  $Gr$ , solutal Grashof number  $Gm$ , magnetic field parameter  $M$ , porous permeability parameter  $K$ , Schmidt number  $Sc$ , heat absorption parameter  $\phi$ , absorption of radiation parameter  $Q_1$ , chemical reaction parameter  $\gamma$ , thermal radiation parameter  $F$  and rarefaction parameter  $h$  on the velocity, temperature and the concentration profiles can be analyzed from Figs. 1–18 and on skin friction coefficient in Tables. 1–3.

In the present study following default parameter values are adopted for computations:  $Gr = 2.0$ ,  $Gm = 2.0$ ,  $M = 1.0$ ,  $K = 0.5$ ,  $h = 0.2$ ,  $Pr = 0.7$ ,  $E = 0.01$ ,  $F = 1.0$ ,  $\phi = 1.0$ ,  $Q_1 = 1.0$ ,  $Sc = 0.6$  and  $\gamma = 0.5$ . All graphs and tables therefore correspond to these values unless specifically indicated on the appropriate graph and table.

Figs. 1 and 2 depict the velocity profiles for cooled Newtonian fluid ( $Gr > 0$ ) and heating Newtonian fluid ( $Gr < 0$ ), respectively. The thermal Grashof number signifies the relative effect of the thermal buoyancy (due to density differences) force to the viscous hydrodynamic force in the boundary layer flow. As seen from this figure that maximum peak value attains for  $Gr = 5.0$  and minimum peak value is observed in the absence of buoyancy force. This is due to the fact that buoyancy force enhances fluid velocity and increase the boundary layer thickness with increase in the value of  $Gr$ . It is observed that an increasing in  $Gr$  leads to an increasing in the value of velocity field. In addition, the curves show that the peak value of velocity increases rapidly near the surface as the value of  $Gr$  increases, and then decays to the free stream velocity. It is interesting to observe that back-flow is reduced by increasing the value of  $Gr$ . No back-flow is observed for  $Gr = -1.0$  and  $Gr = -2.0$ . The effect of solutal Grashof number  $Gm$  on velocity profiles in the boundary layer is depicted in Fig. 3. The solutal Grashof number  $Gm$  defines the ratio of the species buoyancy force to the viscous hydrodynamic force. Similar phenomena is seen in Fig. 3 which shows that the velocity increases with increase in the value of solutal Grashof number  $Gm$ . This is due to the fact that boundary layer thickness increases with increase in the value of  $Gm$ .

The effect of magnetic field on velocity profiles in the boundary layer is depicted in Fig. 4. From this figure it is seen that the velocity starts from minimum value of zero at the surface and increases till it attains the peak value and then starts

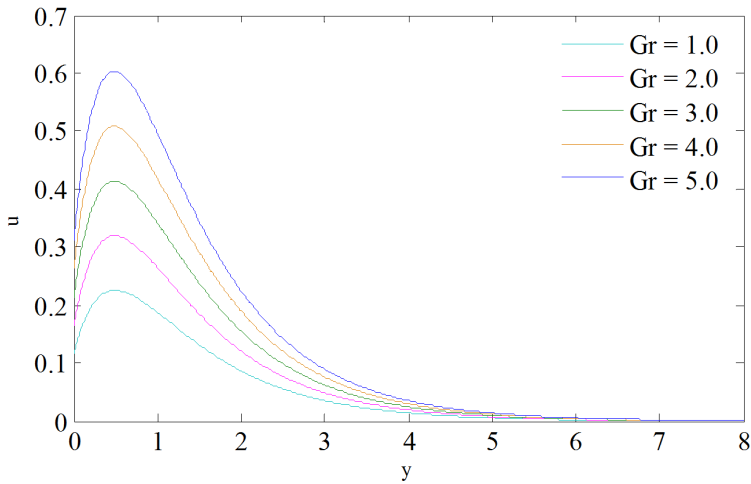


Figure 1: Velocity profile against spanwise coordinate  $y$  for different values of  $Gr$ .

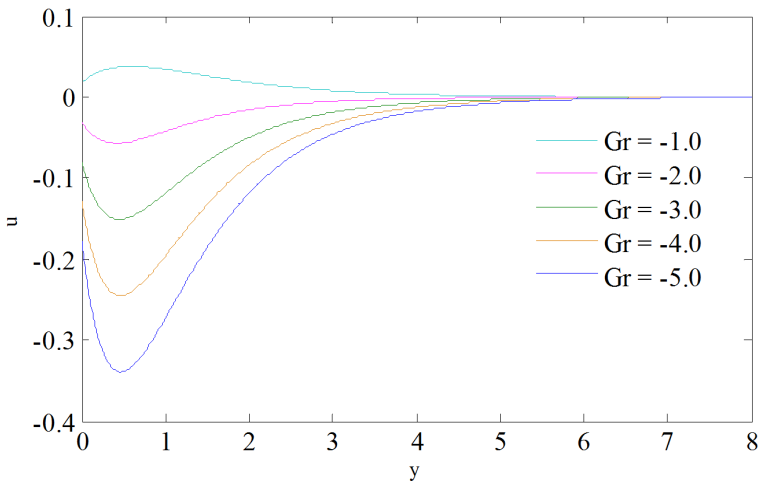


Figure 2: Velocity profile against spanwise coordinate  $y$  for different values of  $Gr$ .

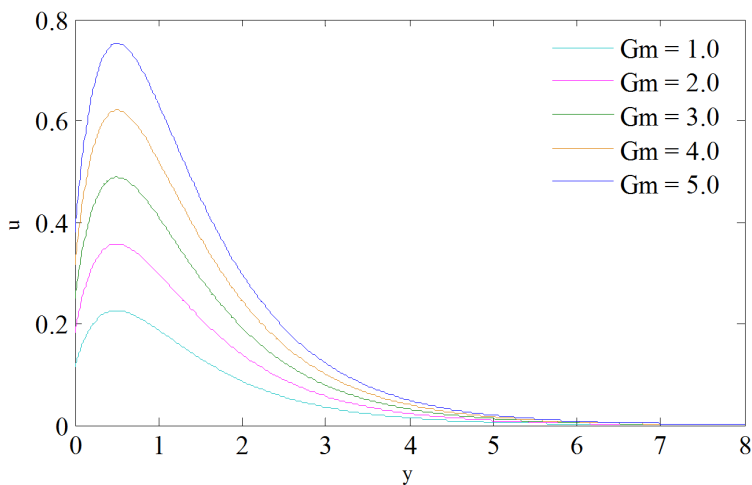


Figure 3: Velocity profile against spanwise coordinate  $y$  for different values of  $Gm$ .

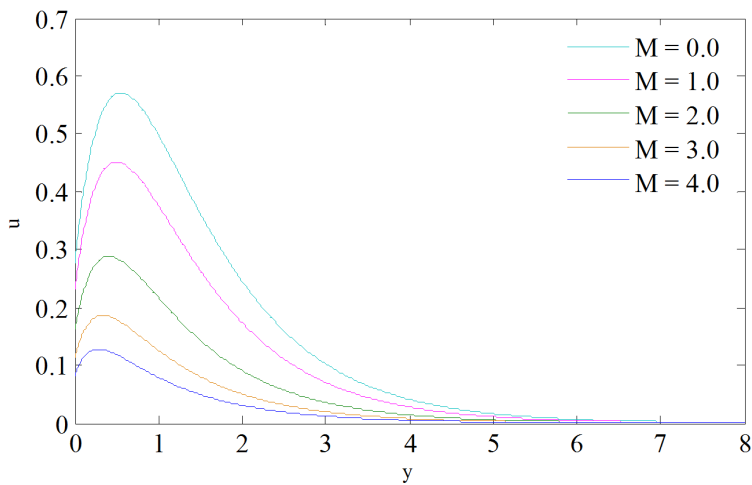


Figure 4: Velocity profile against spanwise coordinate  $y$  for different values of  $M$ .

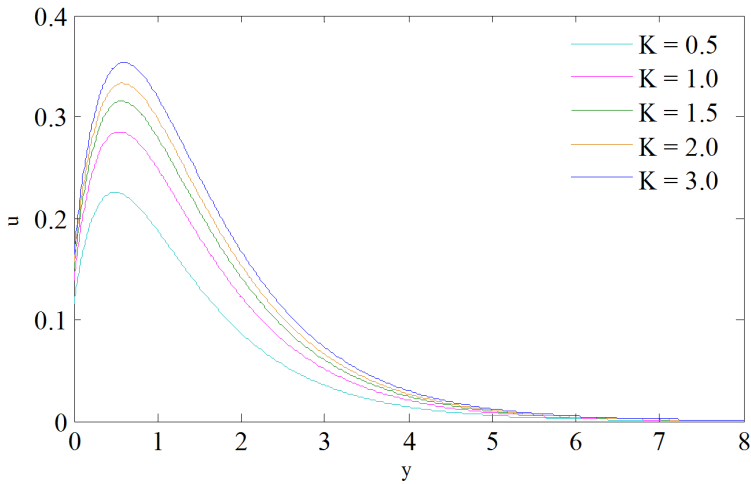


Figure 5: Velocity profile against spanwise coordinate  $y$  for different values of  $K$ .

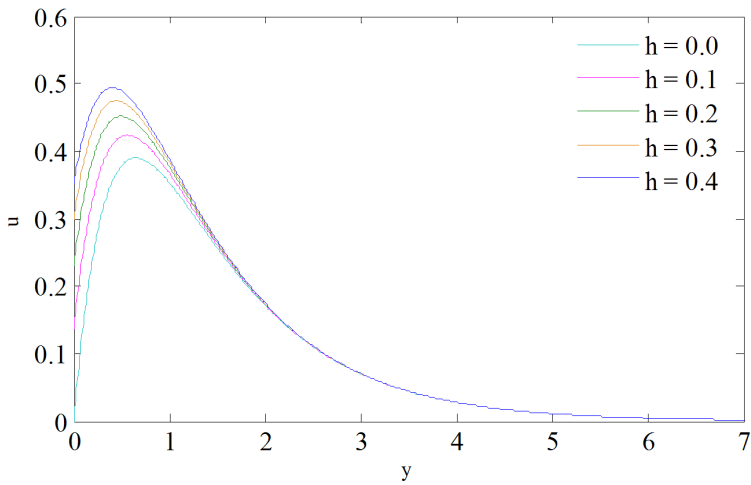


Figure 6: Velocity profile against spanwise coordinate  $y$  for different values of  $h$ .

decreasing until it reaches to the minimum value at the end of the boundary layer for all the values of magnetic field parameter. It is interesting to note that the effect of magnetic field is to decrease the value of the velocity profile throughout the boundary layer. The effect of magnetic field is more prominent at the point of peak value i.e. the peak value drastically decreases with increases in the value of the magnetic field, because the presence of magnetic field in an electrically conducting fluid introduces a force called the Lorentz force, which acts against the flow if the magnetic field is applied in the normal direction, as in the present problem. This type of resisting force slows down the fluid velocity as shown in this figure. The effect the reaction permeability parameter  $K$  on the velocity profiles is shown in Fig. 5. As depicted in this figure, the effect of increasing the value of porous permeability is to increase the value of the velocity component in the boundary layer due to the fact that drag is reduced by increasing the value of the porous permeability on the fluid flow which results in increased velocity.

The variation of velocity profile with rarefaction parameter is represented in Fig. 6. It is evident from this figure that velocity distribution increases rapidly near the plate and then decreases exponentially far away from the plate till it attains the minimum values as  $y \rightarrow \infty$ . The effect of increasing the values of rarefaction parameter is to increase the velocity in the momentum boundary layer with formation of sharp peak near the surface. Thus the effect of  $h$  is more prominently observed very close to the plate which ultimately vanished far away from the plate.

The effect of the radiation parameter  $F$  on the velocity and temperature are shown in Figs. 7 and 8 respectively. The radiation parameter  $F$  defines the relative contribution of conduction heat transfer to thermal radiation transfer. It is obvious that an increase in the radiation parameter results in decreasing velocity within the boundary layer. It is seen from Fig. 8 that the increase of the radiation parameter  $F$  leads decrease the boundary layer thickness and thereby decrease in the value of the heat transfer in the presence of thermal and solutal buoyancy force.

The effect of increasing the value of the heat absorption parameter  $\phi$  is to decrease the boundary layer as shown in Fig. 9, which is as expected due to the fact that when heat is absorbed the buoyancy force decreases which retards the flow rate and thereby giving rise to decrease in the velocity profiles. Fig. 10 has been plotted to depict the variation of temperature profiles against  $y$  for different values of heat absorption parameter  $\phi$  by fixing other physical parameters. From this graph we observe that temperature  $\theta$  decreases with increase in the heat absorption parameter  $\phi$  because when heat is absorbed, the buoyancy force decreases the temperature profile. The opposite trend is observed for the case of increasing the value of the absorption of the radiation parameter due to increase in the buoyancy force which accelerates the flow rate as shown in Fig. 11. Fig. 12 depicts the graph of tem-

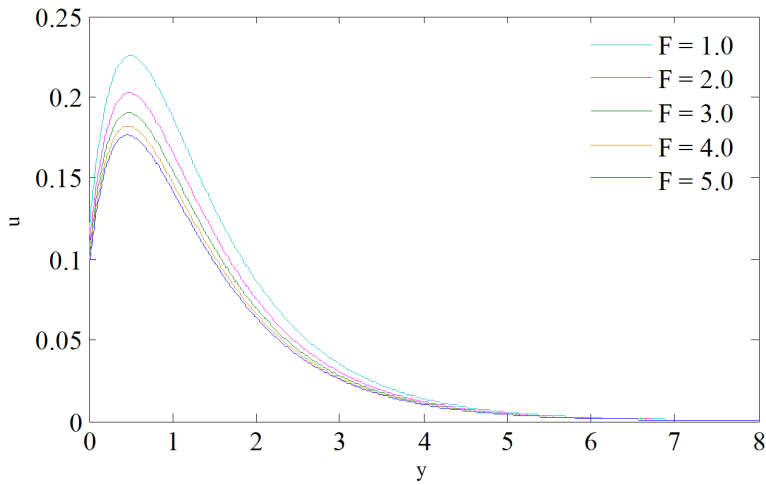


Figure 7: Velocity profile against spanwise coordinate  $y$  for different values of  $F$ .

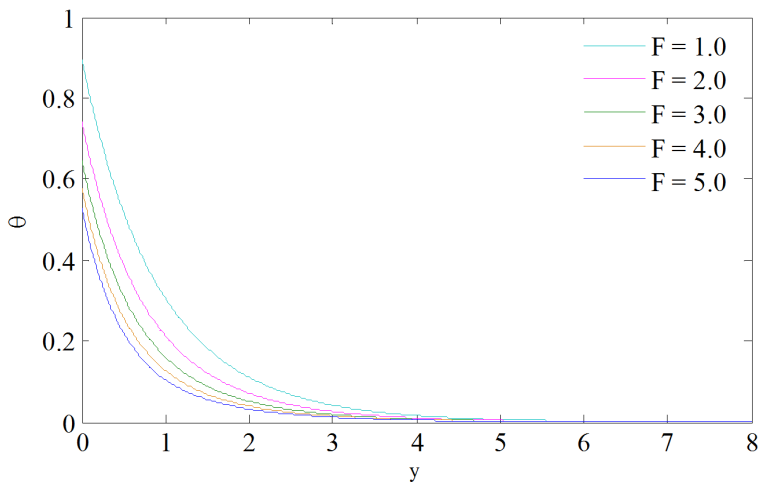


Figure 8: Temperature profile against spanwise coordinate  $y$  for different values of  $F$ .

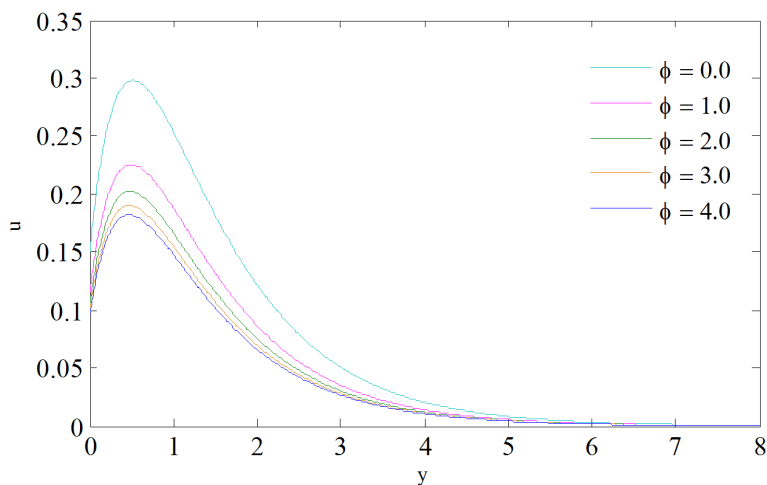


Figure 9: Velocity profile against spanwise coordinate  $y$  for different values of  $\varphi$ .

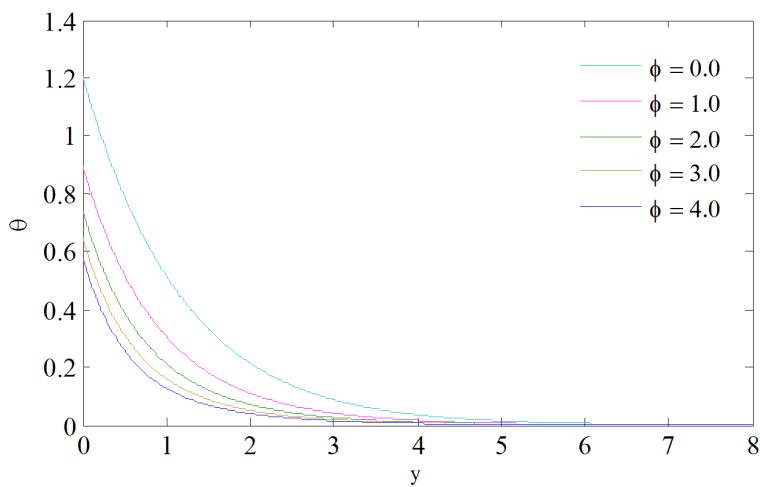


Figure 10: Temperature profile against spanwise coordinate  $y$  for different values of  $\varphi$ .

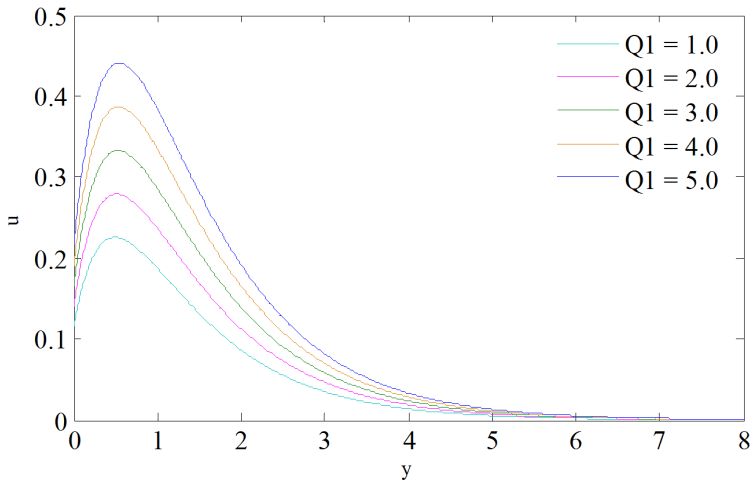


Figure 11: Velocity profile against spanwise coordinate  $y$  for different values of  $Q_1$ .

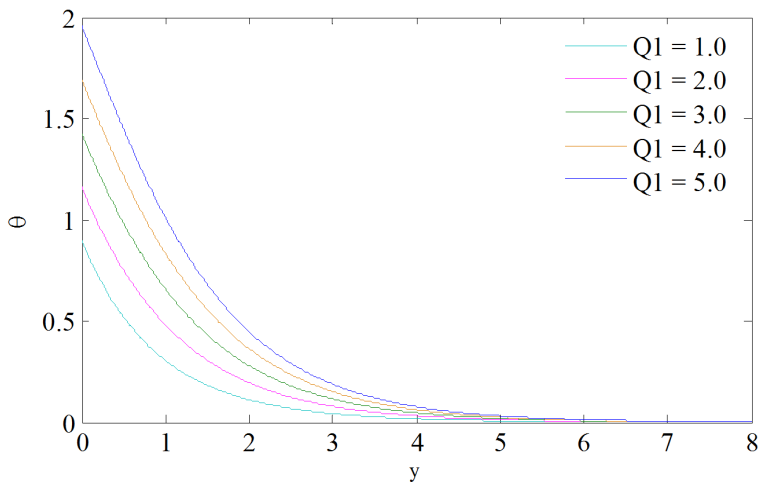


Figure 12: Temperature profile against spanwise coordinate  $y$  for different values of  $Q_1$ .

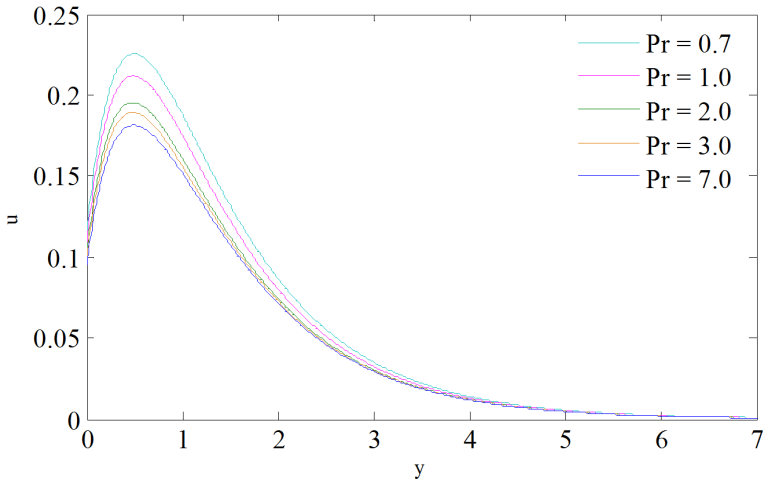


Figure 13: Velocity profile against spanwise coordinate  $y$  for different values of  $Pr$ .

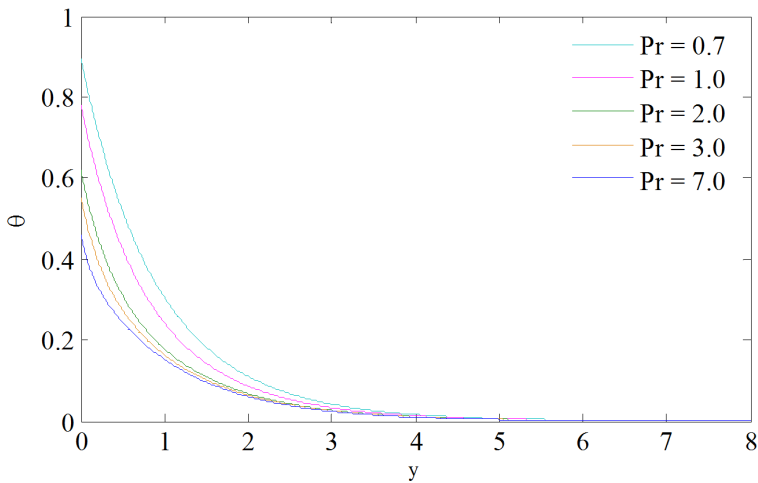


Figure 14: Temperature profile against spanwise coordinate  $y$  for different values of  $Pr$ .

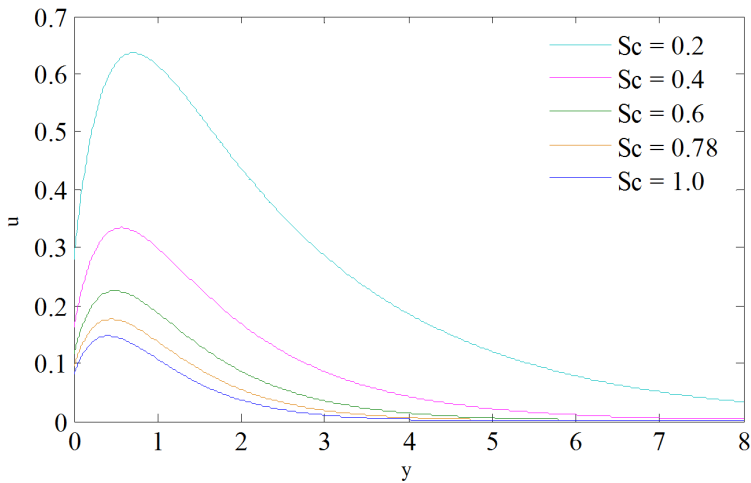


Figure 15: Velocity profile against spanwise coordinate  $y$  for different values of  $Sc$ .

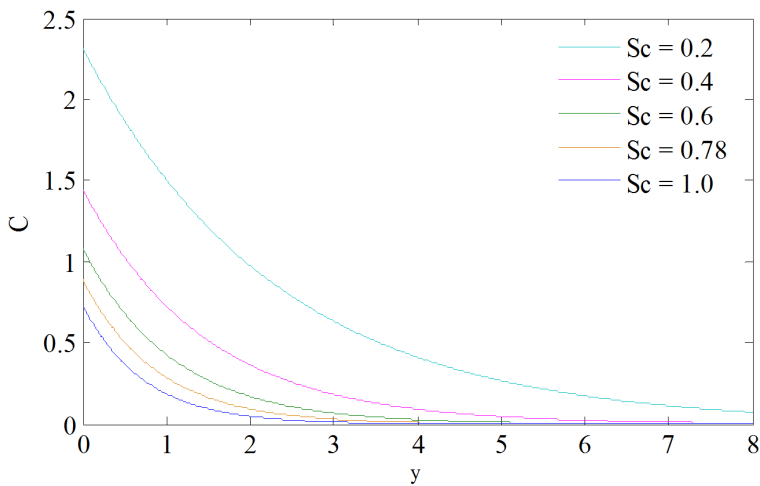


Figure 16: Concentration profile against spanwise coordinate  $y$  for different values of  $Sc$ .

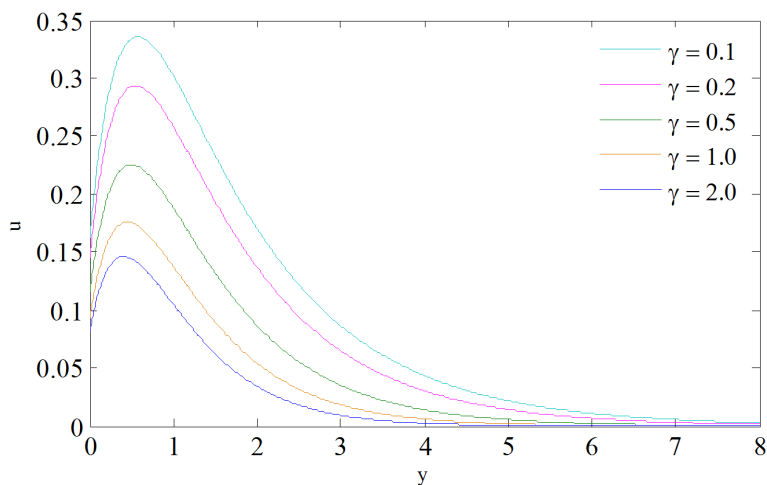


Figure 17: Velocity profile against spanwise coordinate  $y$  for different values of  $\gamma$ .

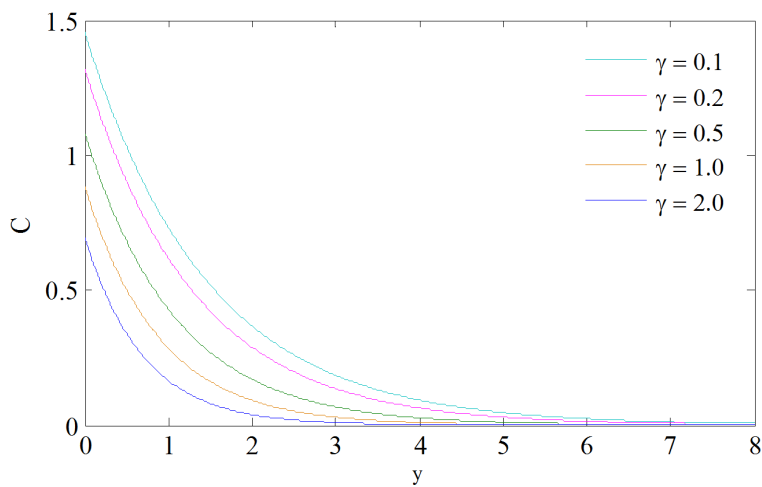


Figure 18: Concentration profile against spanwise coordinate  $y$  for different values of  $\gamma$ .

perature profile  $\theta$  for various values of absorption of radiation parameter  $Q_1$  in the boundary layer. It is seen that the effect of absorption of radiation parameter is to increase temperature in the boundary layer as the radiated heat is absorbed by the fluid which is responsible for increase in the temperature of the fluid very close to the porous boundary layer and its effect diminished far away from the porous boundary.

The velocity of the flow field varies significantly with the variation of the Prandtl number as seen from Fig. 13. It is observed that an increase in Pr leads to rise in the values of velocity. In addition, the curves show that the peak value of velocity decreases rapidly near the plate as Prandtl number increases. Peak velocity is achieved near the plate which decays to the relevant free stream velocity. Fig. 14 shows that the temperature field is found to vary with decrease or increase with variation of the Prandtl number. Curve with  $Pr = 0.7$  represents for air and  $Pr = 7.0$  for water at  $20^\circ C$ . This indicates that the temperature profile for air is more than water. This figure also shows that the temperature for water reduces at a greater speed than for air. Thus it is pointed out that the temperature of the flow field diminishes as the Prandtl number increases, and higher the Prandtl number sharper the reduction in the temperature of the flow field. The Prandtl number defines ratio of momentum diffusivity to thermal diffusivity, so smaller values of Pr are equivalent to increasing the thermal conductivities. Therefore, heat is able to diffuse away from the heated plate more rapidly than for higher values of Pr. Hence for higher values of Prandtl numbers, the boundary layer thickness decreases so the rate of heat transfer is increased. Thus it is observed that increasing Prandtl number results in decrease of the temperature distribution. Thus the buoyancy force due to temperature gradient has the effect of increasing the velocity of the fluid as the Prandtl number is decreased as clearly seen from Fig. 13.

Fig. 15 describes the effect of Schmidt number  $Sc$  on the velocity profiles of the flow field which reveal that the velocity profile decreases with increase in the value of Schmidt number, i.e., the presence of heavier diffusing species has a retarding effect on the velocity of the flow field. The variation of the concentration distribution of the flow field with the diffusion of the foreign species is shown in Fig. 16 for hydrogen ( $Sc = 0.2$ ),  $Sc = 0.4$ , ammonia ( $Sc = 0.78$ ), and  $Sc = 1.0$ . It is observed from this figure that the concentration distribution decreases at all the points of the flow field with increase of the Schmidt number  $Sc$  which shows that heavier diffusing species have greater retarding effect on the concentration distribution of the flow field, due to the fact that the boundary layer thickness greatly decreases with increase in the value of the Schmidt number.

Fig. 17 depicts the effect of chemical reaction parameter  $\gamma$  on the velocity profiles for generative chemical reaction. From this figure, which shows that the velocity

decreases with increasing the rate of chemical reaction  $\gamma$ . Hence increase in the chemical reaction rate parameter leads to a fall in the momentum boundary layer. The effect the reaction rate parameter  $\gamma$  on the species concentration profiles for generative chemical reaction is shown in Fig. 18. It is noticed for the graph that there is marked effect of increasing the value of the chemical reaction rate parameter  $\gamma$  on concentration distribution in the boundary layer. It is clearly observed from this figure that the concentration of species value of 1.0 at vertical plate decreases till it attains the minimum value of zero at the end of the boundary layer and this trend is seen for all the values of reaction rate parameter. Further, it is observed that increasing the value of the chemical reaction decreases the concentration of species in the boundary layer, this is due to the fact that destructive chemical reduces the solutal boundary layer thickness and increases the mass transfer.

In order to verify the accuracy of the present results, we have considered the analytical solutions obtained by Acharya et al. (1968) and computed the numerical results for skin-friction coefficient, local Nusselt number and local Sherwood number. These computed results are tabulated in Table 1. It is interesting to observe from this table that the present results (under some limiting conditions) are in very good agreement with the computed results obtained from the analytical solutions of Acharya et al. (1968), which clearly shows the correctness of the present analytical solutions and computed results.

Table 1: Comparison of present results with those of Acharya et al. (1968) with different values of  $M$  on  $C_{f_x}$ .

Acharya et al. (1968)		Present results ( $h = 0, \varphi = F = 0, Q_1 = 0, \gamma = 0$ )
$M$	$C_{f_x}$	$C_{f_x}$
0.0	2.6899	2.6899
1.0	2.2693	2.2693
2.0	1.6632	1.6632
3.0	1.2519	1.2519
4.0	0.9890	0.9890

Tables 2 and 3 show the effect of thermal Grashof number  $Gr$ , solutal Grashof number  $Gm$ , is magnetic field parameter  $M$ , permeability parameter  $K$ , rarefaction parameter, Prandtl number  $Pr$ , radiation parameter  $F$ , heat source parameter  $\varphi$ , absorption of radiation parameter  $Q_1$ , Schmidt number  $Sc$  and chemical reaction rate parameter  $\gamma$  on skin-friction coefficient  $C_{f_x}$ .

From Table 2, it is seen that the effect of  $Gr$ ,  $Gm$  and  $K$  is to increase skin-friction coefficient  $C_{f_x}$  whereas opposite effect is seen on the values of skin-friction coefficient by increasing the values of  $M$  and  $h$ . It is clearly observed that the values of skin friction coefficient  $C_{f_x}$  decrease with the increase in  $Pr$ ,  $F$  and  $\phi$  and increase in the values of  $Q_1$  (Table 3).

Table 2: Variation of skin friction coefficient  $C_{f_x}$  for different values of physical parameters.

$Gr$	$Gm$	$M$	$K$	$h$	$C_{f_x}$
2.0	2.0	2.0	0.5	0.2	0.8064
4.0	2.0	2.0	0.5	0.2	1.1517
2.0	4.0	2.0	0.5	0.2	1.2697
2.0	2.0	4.0	0.5	0.2	0.4137
2.0	2.0	2.0	1.0	0.2	0.8907
2.0	2.0	2.0	0.5	0.4	0.5865

Table 3: Variation of skin friction coefficient  $C_{f_x}$  for different values of physical parameters.

$Pr$	$F$	$\phi$	$Q_1$	$C_{f_x}$
0.7	2.0	1.0	2.0	1.2144
1.0	2.0	1.0	2.0	1.0490
0.7	3.0	1.0	2.0	1.1183
0.7	2.0	3.0	2.0	1.0588
0.7	2.0	1.0	4.0	1.5458

### 5 Conclusions

In this study, a numerical analysis has been presented about the influence of thermal radiation and a magnetic field on a steady mixed convective boundary layer slip flow (taking into account a homogeneous chemical reaction of first-order, absorption of radiation in the presence of Ohmic dissipation and viscous dissipation). The nonlinear and coupled governing equations have been solved analytically by a perturbation technique. The physical parameters found to affect the fields under consideration are the Grashof number, magnetic field parameter, permeability

parameter, radiation parameter, Prandtl number, absorption of radiation parameter, heat absorption parameter, Schmidt number and chemical reaction parameter. From the computed results the following conclusions are drawn:

The Grashof numbers for heat transfer  $Gr$  and mass transfer  $Gm$  accelerate the flow velocity.

1. The Grashof numbers for heat transfer  $Gr$  and mass transfer  $Gm$  accelerate the flow velocity.
2. The magnetic parameter  $M$  retards the velocity of the flow field at all points due to the magnetic pull of the Lorentz force.
3. The concentration distribution of the flow field decreases at all points as the Schmidt number  $Sc$  increases. This means the heavier diffusing species have a greater retarding effect on the concentration distribution of the flow field.
4. It is found that the velocity as well as concentration decreases with an increase in the chemical reaction parameter.
5. The effect of increasing the values of rarefaction parameter is to increase the velocity in the momentum boundary layer with formation of a sharp peak near the surface.
6. It is found that the velocity as well as temperature decreases with an increase in the heat thermal radiation parameter and source parameter whereas the opposite trend is seen by increasing the values of thermal and absorption of radiation parameter.
7. An increase in the Prandtl number, the Schmidt number, the magnetic parameter, or the radiation parameter leads to a decrease in the value of the skin-friction coefficient, while an increase in the permeability parameter, thermal Grashof number, or the solutal Grashof number leads to an increase in the value of the skin-friction coefficient.

## References

**Abo-Eldahab, E. M.; Abd El-Aziz, M.** (2004): Hall current and Ohmic heating effects on mixed convection boundary layer flow of a micropolar fluid from a rotating cone with power-law variation in surface temperature. *Int. Commun Heat Mass Transfer*, vol. 31, pp. 751–62.

**Abd El-Aziz, M.** (2007): Temperature dependent viscosity and thermal conductivity effects on combined heat and mass transfer in MHD three dimensional flow over a stretching surface with Ohmic heating. *Meccanica*, vol. 42, pp. 375–86.

**Acharya, M.; Singh, L. P.; Dash, G. C.** (1999): Heat and mass transfer over an accelerating surface with heat source in the presence of suction and blowing. *Int. J. Eng. Sci.*, vol. 37, pp. 189–210.

**Acharya, M.; Dash, G. C.; Singh, L. P.** (2000): Magnetic field effects on the free convection and mass transfer flow through porous medium with constant suction and constant heat flux. *Indian J. Pure Appl. Math.*, vol. 31, no. 1, pp. 1-18.

**Aydin, O.; Kaya, A.** (2008): Radiation effect on MHD mixed convection flow about a permeable vertical plate. *Heat Mass Transfer*, vol. 45, pp. 239–46.

**Chaudhary, R. C.; Sharma, B. K.; Jha, A. K.** (2006): Radiation effect with simultaneous thermal and mass diffusion in MHD mixed convection flow. *Rom. J. Phys.*, vol. 51, no. 7–8, pp. 715–27.

**Chen, C. H.** (2004): Combined heat and mass transfer in MHD free convection from a vertical surface with Ohmic heating and viscous dissipation. *Int. J. Eng. Sci.*, vol. 42, pp. 699–713.

**Cogley, A. C.; Vincenty, W. G.; Gilles, E. S.** (1968): Differential approximation for radiation transfer in a non-gray gas near equilibrium. *AIAAJ*, vol. 6, pp. 551–5.

**Ghaly, A. Y.; Seddeek, M. A.** (2004): Chebyshev finite difference method for the effect of chemical reaction, heat and mass transfer on laminar flow along a semi-infinite horizontal plate with temperature dependent viscosity. *Chaos Solitons Fractals*, vol. 19, pp. 61–70.

**Hayat, T.; Abbas, Q.; Asghar, S.; Siddiqui, A. M.; Farid, T.; Murtaza, G.** (2002): Flow of an elastico-viscous fluid past an infinite wall with time-dependent suction. *Acta Mech*, vol. 153, pp. 133–45.

**Hossain, M. A.** (1992): Viscous and joule heating effects on MHD free convection flow with variable plate temperature. *Int. J. Heat Mass Transfer*, vol. 35, pp. 3485–7.

**Hossain, M. A.; Takhar, H. S.** (1996): Radiation effect on mixed convection along a vertical plate with uniform surface temperature. *Heat Mass Transfer*, vol. 31, pp. 243–8.

**Kandasamy, R.; Perisamy, K. K.; Prabhu, S.** (2005): Chemical reaction, heat and mass transfer on MHD flow over a vertical stretching surface with heat source and thermal stratification effects. *Int. J. Heat Mass Transfer*, vol. 48, pp. 4557–61.

**Khair, K. R.; Bejan, A.** (1985): Mass transfer to natural convection boundary layer flow driven by heat transfer. *Int. J. Heat Mass Transfer*, vol. 107, pp. 369–76.

**Lin, H. T.; Wu, C. M.** (1995): Combined heat and mass transfer by laminar natural convection from a vertical plate. *Heat Mass Transfer*, vol. 30, pp. 369–76.

**Sharma, P. K.; Chaudhury, R. C.** (2003): Effect of variable suction on transient

flow convective viscous incompressible flow past a vertical plate with periodic temperature variations in slip flow regime. *Emirates J. Eng. Sci.*, vol. 8, pp. 33–8.

**Reddy, M. G.; Reddy, N. B.** (2011): Mass Transfer and Heat Generation Effects on MHD Free Convection Flow past an Inclined Vertical Surface in a Porous Medium. *Journal of Applied Fluid Mechanics*, vol. 4, pp. 7-11.

**Reddy, M. G.** (2012): Thermal radiation and viscous dissipation effects on MHD marangoni convection flow over a permeable flat surface with heat generation/absorption. *British Journal of Engineering & Technology*, vol. 1, pp. 17-32.

**Reddy, M. G.** (2013): Influence of thermal radiation, viscous dissipation and hall current on MHD convection flow over a stretched vertical flat plate. *Ain Shams Engineering Journal*, vol. 5, pp. 169-175.

**Reddy, M. G.** (2013): Chemically reactive species and radiation effects on MHD convective flow past a moving vertical cylinder. *Ain Shams Engineering Journal*, vol. 4, pp. 879-888.

**Reddy, M. G.** (2014): Thermal radiation and chemical reaction effects on MHD mixed convective boundary layer slip flow in a porous medium with heat source and Ohmic heating. *Eur. Phys. J. Plus*, vol. 129, pp. 41.

**Seddeek, M. A.** (2002): Effects of radiation and variable viscosity on a MHD free convection past a semi-infinite flat plate with an aligned magnetic field in the case of unsteady flow. *Int. J. Heat Mass Transfer*, vol. 45, pp. 931–5.

**Yin, K. A.** (1999): Free convection effect on MHD coupled heat and mass transfer of a moving permeable vertical surface. *Int. Commun Heat Mass Transfer*, vol. 26, pp. 95–104.

**Appendix A**

$$\begin{aligned}
 A_1 &= \frac{Sc + \sqrt{Sc^2 + 4Sc}}{2}, & A_2 &= \frac{Pr + \sqrt{Pr^2 + 4Pr(F + \phi)}}{2}, \\
 A_3 &= \frac{-Pr Q_1}{A_1 (A_1^2 - Pr A_1 - Pr(F + \phi))}, & A_4 &= \frac{1 + \sqrt{1 + 4p}}{2}, \\
 A_5 &= \frac{-Gr \left( \frac{1 - A_1 A_3}{A_2} \right)}{A_2^2 - A_2 - p}, & A_6 &= \frac{-\left( Gr A_3 + Gm/A_1 \right)}{A_1^2 - A_1 - p}, \\
 A_7 &= \frac{-(A_5 (1 + hA_2) + A_6 (1 + hA_1))}{(1 + hA_4)}, & A_8 &= \frac{-Pr A_6^2 (A_1^2 + M^2)}{4A_1^2 - 2Pr A_1 - Pr(F + \phi)}, \\
 A_9 &= \frac{-Pr A_5^2 (A_2^2 + M^2)}{4A_2^2 - 2Pr A_2 - Pr(F + \phi)}, & A_{10} &= \frac{-Pr A_7^2 (A_4^2 + M^2)}{4A_4^2 - 2Pr A_4 - Pr(F + \phi)},
 \end{aligned}$$

$$A_{11} = \frac{-2\Pr A_5 A_6 (A_1 A_2 + M^2)}{(A_1 + A_2)^2 - \Pr(A_1 + A_2) - \Pr(F + \varphi)},$$

$$A_{12} = \frac{-2\Pr A_6 A_7 (A_1 A_4 + M^2)}{(A_1 + A_4)^2 - \Pr(A_1 + A_4) - \Pr(F + \varphi)},$$

$$A_{13} = \frac{-2\Pr A_5 A_7 (A_2 A_4 + M^2)}{(A_2 + A_4)^2 - \Pr(A_2 + A_4) - \Pr(F + \varphi)},$$

$$A_{14} = -(2A_1 A_8 + 2A_2 A_9 + 2A_4 A_{10} + A_{11}(A_1 + A_2) + A_{12}(A_1 + A_4) + A_{13}(A_2 + A_4)),$$

$$A_{15} = \frac{-GrA_{14}}{A_2^2 - A_2 - p}, \quad A_{16} = \frac{-GrA_8}{4A_1^2 - 2A_1 - p}, \quad A_{17} = \frac{-GrA_9}{4A_2^2 - 2A_2 - p},$$

$$A_{18} = \frac{-GrA_{10}}{4A_4^2 - 2A_4 - p}, \quad A_{19} = \frac{-GrA_{11}}{(A_1 + A_2)^2 - (A_1 + A_2) - p},$$

$$A_{20} = \frac{-GrA_{12}}{(A_1 + A_4)^2 - (A_1 + A_4) - p}, \quad A_{21} = \frac{-GrA_{13}}{(A_2 + A_4)^2 - (A_2 + A_4) - p},$$

$$A_{22} = A_{19}(A_1 + A_2), \quad A_{23} = A_{20}(A_1 + A_4),$$

$$A_{24} = A_{21}(A_2 + A_4), \quad A_{25} = 2(A_1 A_{16} + A_2 A_{17} + A_4 A_{18}),$$

$$A_{26} = A_{15} + A_{16} + A_{17} + A_{18} + A_{19} + A_{20} + A_{21},$$

$$A_{27} = \frac{-(h(A_2 A_{15} + A_{25} + A_{22} + A_{23} + A_{24}) + A_{26})}{(1 + hA_4)}.$$